CHALMERS
UNIVERSITY OF TECHNOLOGY

Upgrading of fast pyrolysis bio-oils to renewable hydrocarbons using slurry- and fixed bed hydroprocessing

Fuel Processing Technology 253 (2024) 108009

Contents lists available at ScienceDirect

Fuel Processing Technology

journal homepage: www.elsevier.com/locate/fuproc

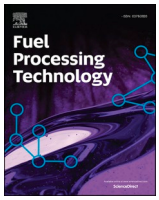

Upgrading of fast pyrolysis bio-oils to renewable hydrocarbons using slurry- and fixed bed hydroprocessing

Niklas Bergvall [a,*], You Wayne Cheah [b], Christian Bernlind [a], Alexandra Bernlind [a], Louise Olsson [b], Derek Creaser [b], Linda Sandström [a], Olov G.W. Öhrman [c]

[a] Research Institutes of Sweden AB, Box 857, SE-501 15 Borås, Sweden
[b] Competence Centre for Catalysis, Department of Chemical Engineering, Chalmers University of Technology, SE-41 296 Gothenburg, Sweden
[c] Preem AB, Box 48084, SE-418 23 Gothenburg, Sweden

ARTICLE INFO

Keywords:
Pyrolysis
Hydroprocessing
Slurry
Biofuel
Deoxygenation
Renewable

ABSTRACT

Liquefaction of lignocellulosic biomass through fast pyrolysis, to yield fast pyrolysis bio-oil (FPBO), is a technique that has been extensively researched in the quest for finding alternatives to fossil feedstocks to produce fuels, chemicals, etc. Properties such as high oxygen content, acidity, and poor storage stability greatly limit the direct use of this bio-oil. Furthermore, high coking tendencies make upgrading of the FPBO by hydrodeoxygenation in fixed-bed bed hydrotreaters challenging due to plugging and catalyst deactivation. This study investigates a novel two-step hydroprocessing concept; a continuous slurry-based process using a dispersed NiMo-catalyst, followed by a fixed bed process using a supported NiMo-catalyst. The oil product from the slurry-process, having a reduced oxygen content (15 wt%) compared to the FPBO and a comparatively low coking tendency (TGA residue of 1.4 wt%), was successfully processed in the downstream fixed bed process for 58 h without any noticeable decrease in catalyst activity, or increase in pressure drop. The overall process resulted in a 29 wt% yield of deoxygenated oil product (0.5 wt% oxygen) from FPBO with an overall carbon recovery of 68%.

1. Introduction

The depletion of fossil-derived resources and the alarming environmental issues associated with its use have prompted the search for renewable alternatives to create a sustainable society. Sweden has ambitiously outlined Climate goals aiming to achieve net zero greenhouse gas (GHG) emissions by 2045 and, subsequently, achieve negative emissions [1]. In terms of decarbonizing the transportation sector, Sweden has set a goal to reduce the emissions from the transport sector (excluding domestic aviation), with 70% by 2030 [1]. To achieve this, various solutions and joint efforts in improving the existing renewable fuel production capabilities and also exploring and expanding the current renewable feedstocks portfolio are needed.

Fast pyrolysis bio-oil (FPBO), a viscous and heavy bio-crude resulting from the fast pyrolysis process of solid biomass, has the potential for further upgrading to obtain liquid fuel-like and chemical-like products. During the fast pyrolysis of biomass, solid biomass is converted into liquid bio-oil, solid char, and non-condensable gases at conditions such as temperature ranging from 350 to 525 °C, an inert atmosphere, with short residence time (< 1 s), and rapid quenching of the vapors [2]. The composition of FPBO depends largely on the biomass source and the bio-oil usually consists of a wide spectrum of compound classes such as aliphatics, phenolic compounds, ketones, aldehydes, sugars, esters, carboxylic acids, alcohols, and water [3]. The high oxygen content in FPBO contributes to its detrimental properties such as corrosiveness, high viscosity, low heating value, and thermal instability [4]. Catalytic pyrolysis has been studied as an alternative to fast pyrolysis and although it does produce a pyrolysis oil with improved properties, the recovery of carbon to the oil is reduced and alkali metals present in the biomass ash typically deposit on the catalysts and eventually lead to catalyst deactivation [5]. Hence, a refining process that can stabilize the bio-oil and also reduce the heteroatom content by means of hydrotreatment is needed for further applications and improved economic performance of fast pyrolysis plants [6].

Several efforts have been made to hydroprocess FPBO using various concepts [7], such as 1-stage continuous fixed-bed [8], 2-stage fixed-bed with mild hydrotreating followed by high-temperature hydrocracking [9,10], and a pre-derivatization step followed by hydrotreatment in a

* Corresponding author.
E-mail address: niklas.bergvall@ri.se (N. Bergvall).

https://doi.org/10.1016/j.fuproc.2023.108009
Received 2 October 2023; Received in revised form 23 November 2023; Accepted 24 November 2023
Available online 12 December 2023

fixed-bed hydrotreater [11]. Plugging and catalyst deactivation are challenging issues for fixed bed hydrotreating of FPBO [7,12,13], despite adding specific stabilization steps with lower temperatures and different catalysts [10,14,15]. A comprehensive review recently outlined the development efforts of the VTT Technical Research Centre of Finland, Ltd. in fast pyrolysis technology discussing its commercialization, upgrading, applications of pyrolysis products, and method development for process improvements, also further highlighting the need for more work to be done at the pilot scale before implementation in a complex refinery [16]. Yang et al. also concluded that most studies of hydrodeoxygenation of bio-oils are performed using model compounds, even though raw bio-oils should preferably be used, as results from model compound studies do not necessarily scale well to processing of the very complex crude bio-oils [17]. Aside from upgrading pure FPBO, co-processing of FPBO with fossil feedstocks in fixed bed reactors has also been investigated, for example by Santosa et al. who reported the continuous co-processing of 5–25% FPBO and catalytic FPBO with fossil vacuum gas oil (VGO) in a bench-scale fixed bed hydrotreater [18]. Their study highlights that the instability of raw FPBO easily leads to reactor plugging also during co-processing and that, moreover, catalytic pyrolysis can result in a more stable pyrolysis oil, which facilitates the fixed bed processing. However, the research on co-processing of pyrolysis oils with fossil feedstocks is still quite limited, as pointed out in a recent review [19].

As one remedy to the challenges with hydroprocessing FPBO, slurry-based processing emerges as a feasible technology since such a process is inherently resistant to plugging problems, and the catalyst can be continually withdrawn from, and recirculated to the reactor. In our previous work with this concept, we demonstrated co-hydroprocessing of FPBO (0 or 20 wt%) with vacuum residue (at 50 wt%) and vacuum gas oil (VGO) in a continuous slurry-process process using an oil-soluble molybdenum precursor to generate a dispersed catalyst in-situ [20]. The trials showed successful integration of FPBO during the continuous processing of fossil feeds, with a low coke yield (~ 1 wt%) and high deoxygenation activity. Subsequently, in further work, FPBO was co-processed with VGO (20:80 wt% ratio) in the same pilot slurry hydroprocessing plant in a continuous operation mode [21,22]. Nearly complete deoxygenation (~94%) was achieved at 410 °C reaction temperature and 2 h residence time, or at 435 °C and 1 h residence time [21]. In these settings the recovery of biogenic carbon to the oil products was 53–56 wt%, although the study also highlights the challenges with accurately determining the recovery of biogenic carbon in co-processing. Slurry phase continuous mode co-processing of FPBO with fossil feedstock (light cycle oil, LCO) using an unsupported MoS_2 catalyst has also been studied by Zhang et al. [23]. In their work the FPBO was fed to the reactor as a bio-oil-in-LCO microemulsion. Up to 90% deoxygenation was achieved with low coke formation and biogenic carbon yields to oil phase products from 64 to 71%, along with H_2 consumptions of 24 to 54 g H_2 per kg processed bio-oil.

Besides FPBO, challenging solid bio-feedstocks like Kraft lignin have also been upgraded in a slurry-process by processing with VGO as a carrier liquid, producing stabilized bio-crudes that can be further processed in existing refinery infrastructures [24]. The study showed that superior results can be achieved by feeding cold lignin into a hot slurry hydroprocessing reactor, compared to slowly heating lignin to reaction temperature (such as in batch experiments), since lignin tends to repolymerize at low temperatures (~250 °C). Coke formation at the reactor inlet of fixed bed hydroprocessing reactors is also a known issue for FPBO since it tends to undergo polymerization reactions at similar temperatures [12,13]. Feeding directly into a hot slurry reactor has been argued to be a solution also in this case since the feed will then be very quickly heated to the reaction temperature by dispersing in the hot slurry reactor [20].

In a recent study by Dimitriadis et al., the authors presented a whole production chain covering the production of FPBO from agricultural residue (straw) via fast pyrolysis, followed by stabilization of the resulting FPBO (without co-feed) in a continuous slurry hydrocracking pilot plant (the same as used in this work) [25]. The stabilized FPBO then underwent hydrotreatment in a continuous fixed bed reactor, producing a deoxygenated oil product, fully miscible with fossil feedstocks, that can be integrated into current refinery infrastructure [26]. However, catalyst deactivation and plugging problems were still very much a reality in the fixed bed process. Even though the stabilization in the slurry-process step did lead to improvements, the FPBO was apparently not sufficiently stabilized. The aim of this work is to first hydroprocess FPBO in a slurry-process at more severe reaction conditions to try to achieve a higher degree of stabilization to facilitate downstream hydroprocessing in a fixed bed reactor, with the ultimate goal to find ways to replace fossil feedstocks with renewable counterparts.

In this study, we report a pilot-scale FPBO two-step hydroprocessing concept that first involves the continuous stabilization of the FPBO in a slurry-process with a NiMoS dispersed catalyst, followed by hydrotreating of the stabilized FPBO (slurry-product) in a fixed bed reactor. The slurry-product and also the hydrotreated end-product were analyzed thoroughly using several techniques such as elemental composition, titrations, ^{1}H nuclear magnetic resonance (NMR), ^{31}P NMR, ^{13}C NMR, GC-Simdist, thermogravimetric analysis (TGA), and two dimensional (2D) GC × GC–MS-FID, to better understand the chemical properties of the obtained renewable liquid hydrocarbons. The available literature on continuous modes of upgrading neat FPBO is scarce, and on slurry upgrading of neat FPBO even scarcer, making this study a unique contribution to the scientific community.

2. Experimental

2.1. Raw materials

The FPBO used in this study was a commercially available product obtained from fast pyrolysis of lignocellulosic feedstock and its properties are presented in Table 1. Properties are given for the FPBO as it was used (including water) but concentrations of carbon, hydrogen, and oxygen are also presented on a dry basis.

The NiMoS dispersed catalyst used in the slurry-process was synthesized using a hydrothermal method reported in our previous work [27]. In a typical synthesis, ammonium molybdate tetrahydrate (1.15 g) was used as the Mo precursor, nickel (II) nitrate hexahydrate as the Ni precursor, and thiourea (4.25 g) as the S precursor, and all reactants were dissolved in 180 mL Milli-Q water. The Ni/Mo mole ratio was kept at 0.5. The pH of the solution was also adjusted to 0.8 using HCl (35 wt %). This solution was then transferred to a 300 mL Teflon-liner. After filling the liner with the dissolved solution of precursors, the liner was closed with the Teflon lid and placed in a stainless-steel autoclave. The autoclave was then sealed and heated in an oven at 200 °C for 12 h. The as-synthesized catalyst was then filtered and washed first with Milli-Q

Table 1
Properties of the FPBO.

Property	Method	As received	Dry
Carbon	ASTM D591	46.1 wt%	58.6 wt%
Hydrogen	ASTM D591	6.8 wt%	5.6 wt%
Nitrogen	ASTM D591	0.00 wt%	–
Sulfur	ENISO20884	28.4 ppm	–
Oxygen (by difference)	ASTM D591	47.1 wt%	35.8 wt%
Water	ASTM E203	21.2 wt%	0 wt%
Density	EN ISO 12185	1.2 kg/L	–
Solids content	ASTM D7579	0.00 wt%	–
Ash content	EN ISO 6245	0.00 wt%	–
Kinematic Viscosity (40 °C)	ASTM D445	28.1 cSt	–
Aliphatic OH	^{31}P NMR	4.0 mmol/g	–
Phenol OH	^{31}P NMR	2.3 mmol/g	–
COOH	^{31}P NMR	0.8 mmol/g	–
Carbonyls	ASTM E3146-18a	4.2 mmol/g	5.3 mmol/g
Total Acid Number	ASTM D664	1.2 mmol/g	1.5 mmol/g

water, followed by absolute ethanol. After the washing, the catalyst was dried in an oven at 50 °C under vacuum overnight. The slurry catalyst was used in the slurry-process without any pre-treatment step. The specific surface area of the slurry catalyst was 49.3 m^2/g, with a total pore volume of 0.224 cm^3/g and average pore size of 11.52 nm. The detailed composition and physicochemical properties of the slurry catalyst can be found in our previous work [27]. The catalyst used in the fixed bed (FB) experiment were nickel-molybdenum doped pellets on δ–alumina (HDC-10) from Hulteberg Chemistry & Engineering.

2.2. Slurry processing

A Slurry Hydrocracking pilot plant, situated in Piteå, Sweden, and owned by RISE Research Institute of Sweden, was used in the first processing step of the FPBO. The pilot plant (Fig. 1) features a stirred tank reactor with a total net volume of 2.6 L. The experiment started with the reactor filled with 1.67 g of slurry-catalyst and 500 g hexadecane (which unlike the FPBO is inert during the initial heating of the reactor). After inertizing and leak testing the system, it was pressurized with H_2 to the planned reaction pressure of 100 bars and heated at 200 °C/h to a liquid temperature of 410 °C. During the heating phase and throughout the following experiment, the reactor was stirred at 1340 rpm and continuously fed with 1800 NL/h H_2. Once the planned reaction temperature of 410 °C was reached, a continuous feed of 1 L/h of FPBO, mixed with the slurry catalyst to a concentration of 0.33 wt%, was started and maintained throughout the rest of the experiment (resulting in an average residence time of 2.6 h and a Liquid Hourly Space Velocity (LHSV) of 0.385 h^{-1}). The slurry was fed together with the H_2 to the bottom of the reactor directly into the hot and turbulent reactor interior, which resulted in an instant heating of the FPBO to the reaction temperature (410 °C).

During the experiment, liquid product and gas were continually withdrawn from the top of the reactor and directed to a High-Pressure High-Temperature (HP-HT) separator where water and volatile organic compounds were evaporated, and the remaining product was withdrawn through the bottom as a Heavy Product (naturally containing the catalyst and any other solids particles). The compounds evaporated from the HP-HT separator were directed (via a pressure decrease to around 10 bars) to a Low-Pressure Low-Temperature (LP-LT) separator. There the product separated gravimetrically into a Water Product and a Light Oil Product (insoluble in the Water Product), which were withdrawn into separate product tanks. The gas stream, after passing through a condenser (15 °C) that sent any condensed compounds back to the LP-LT separator, left the system. The mass flow of the gas stream was continually measured using a Coriolis mass flow meter and analyzed by a micro-GC with dual thermal conductivity detectors (TCD). The compounds quantified by the micro-GC were H_2, CO, CO_2, and C_1-C_3 hydrocarbons. Gas samples were also collected in bags to analyze the concentration of C_4 and C_5 hydrocarbons in another GC equipped with a flame ionization detector (FID). The feed tank and all three product tanks were positioned on scales to enable continuous monitoring of the masses and calculation of the mass balances.

The HP-HT separator was heated to 250 °C at the start of the experiment but after some time reached a temperature of around 280 °C only from the hot flow of products from the reactor. Despite the high temperature, not all water was successfully evaporated in the HP-HT separator, and some remained in the Heavy Product. The heavy product tank was emptied around 3.75 h after initiating feeding of slurry to the reactor. The collected product was then separated into three phases; an oil phase at the bottom, a water phase, and another oil phase on top (which later was concluded to consist primarily of hexadecane). Feeding of slurry was continued for another 4 h and the Heavy Product collected after this time consisted of only two phases; water in the bottom and oil on the top (the water phase had a slightly higher density of 1.03 g/mL, versus 1.027 g/mL for the oil phase). The two phases of the Heavy Product were separated by centrifugation and decanting (22.5 wt% water phase of the total mass) and finally dewatered in a rotary evaporator (ca 85 °C and 15 mbar) to remove the last water (the centrifugated oil phase still contained 5.8 wt% water after decanting). Some organic products were also evaporated along with the water during the dewatering, but this organic phase was recovered and returned to the Heavy Oil Product. The two resulting Heavy Oil Products (not including the hexadecane phase) were mixed with the Light Oil Product, filtered with a 10–20 μm filter, and used in the downstream refining in the fixed bed process (FB-process). The mass balance for the slurry-process was calculated during the last 4 h of the experiments, when the conditions were the most stable.

2.3. Fixed bed (FB) processing

A stainless-steel reactor was packed according to Fig. 2, where the catalyst consisted of approximately equal quantities of two milled and sieved fractions of the catalyst, 1.40–2.00 mm and 280 μm – 1.00 mm.

The reactor bed was dried under a stream of nitrogen at 10 bar during a temperature ramp up to 250 °C. Sulfidation of the catalyst was subsequently performed at 70 bar H_2 pressure by pumping in commercially available hydrogenated vegetable oil (HVO) mixed with 4 wt% dimethyl disulfide (DMDS), corresponding to 1.5% S by weight, while increasing the reactor temperature from 150 to 350 °C by 15 °C/min and then maintaining 350 °C for 4 h. The hydrotreatment reaction was then

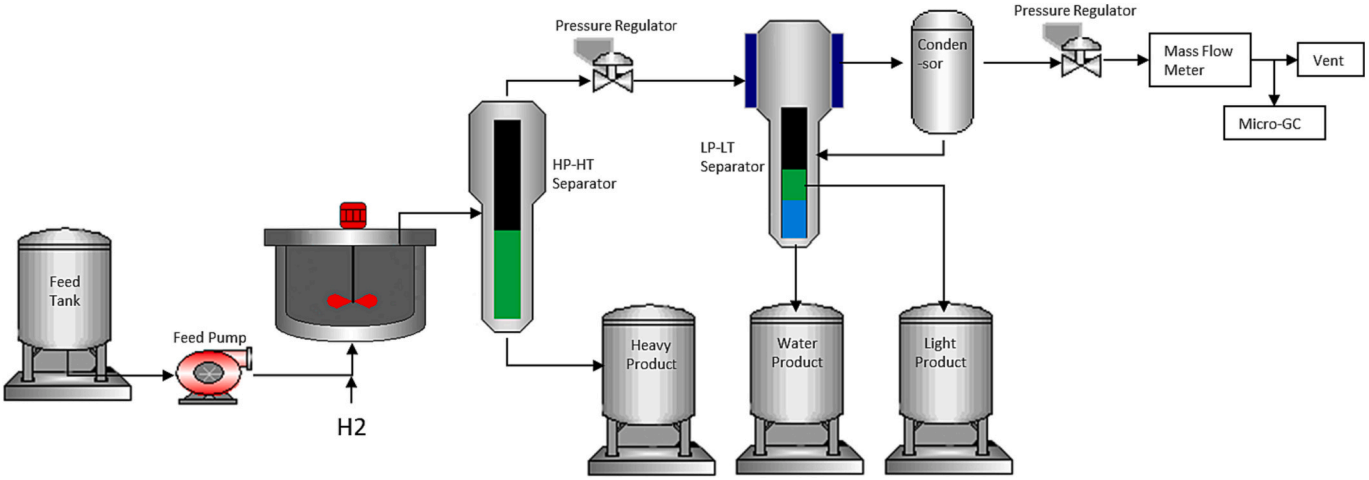

Fig. 1. Schematic representation of the slurry process.

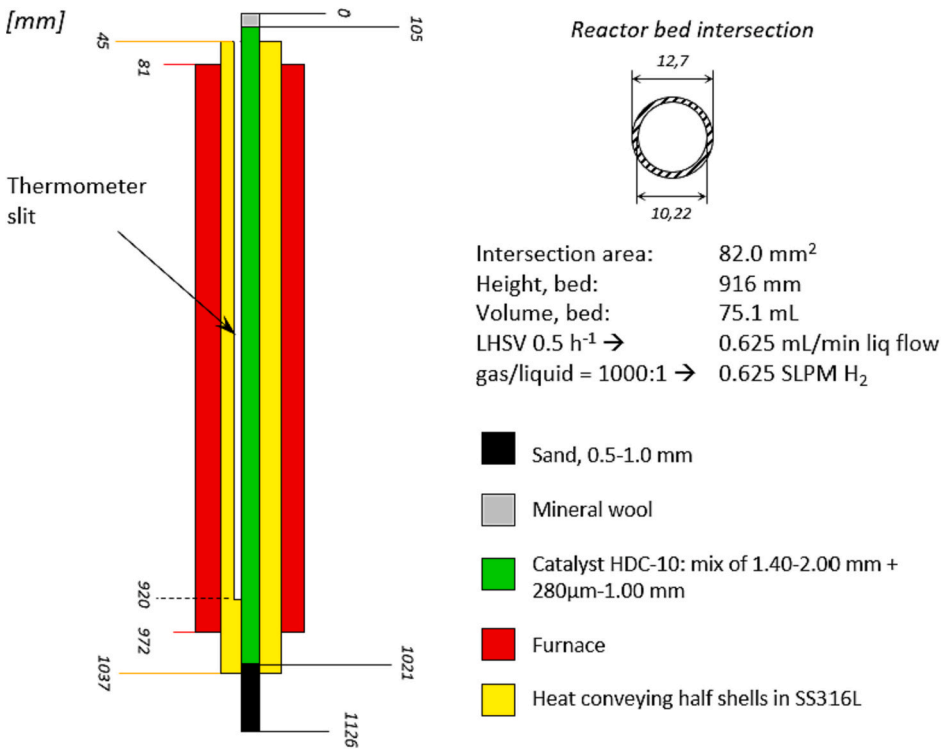

Fig. 2. Properties of the fixed bed reactor.

carried out for the slurry-product (with an addition of 1 wt% DMDS) at 80 bar H_2 with a liquid flow corresponding to a LHSV of 0.5 h^{-1} and a gas-to-oil volumetric feed ratio of 1000:1. The reaction temperature was maintained at 380 °C, aside from a point near the end of the experiment when the temperature was temporarily decreased to 340 °C, before again being increased to 380 °C. The pressure, temperature, gas flow, and liquid flow profiles over the course of the hydrotreatment can be found in Supporting Information, Fig. S1. During the experiment, thirteen liquid samples were collected, of which fractions 4, 11, 12, and 13 were analyzed in more depth. Descriptions of these four samples obtained from the fixed-bed hydrotreatment are as follows: **Sample 4** was the liquid product collected after hydrotreatment at 380 °C, when there should be no traces of the HVO left in the product; **Sample 11** was the liquid product collected after hydrotreatment at 380 °C, before the temperature was decreased; **Sample 12** was the liquid collected after hydrotreatment at 340 °C; and **Sample 13** was the liquid collected after hydrotreatment at 380 °C, after being increased again from 340 °C. Each sample was collected over a period of ca 3–6 h, immediately followed by another sampling period (Supporting Information, Fig. S1). The period during which Sample 12 was collected started with an immediate decrease in temperature from 380 °C to 340 °C and the temperature (measured on the outside of the reactor) reached the lower temperature setting after ca 45 min. Sample 12 was then collected for another 5 h at the reduced temperature. The inside temperature of the reactor may have taken some additional time to reach the reduced temperature, although the reactor diameter is small, and this time is expected to be short. Consequently, it is very likely that the majority of Sample 12 was produced at interior reactor temperature of 340 °C.

The gas leaving the process was measured by a mass flow meter and analyzed by and a Hiden quantitative gas analyzer (H_2, H_2S, C_1-C_4, and CO_2). Unfortunately, the mass flow meter showed erroneous values during the run, which underestimated the gas production and, in turn, overestimated the H_2-consumption. However, since the feed contained 1 wt% DMDS, the concentration of H_2S in the gas stream (only originating from the DMDS since there were no other sulfur sources in the feed) could be used to accurately calculate the total mass flow of gas from the system. In calculating the mass balance, the yields of H_2S and CH_4 obtained from the hydrogenation of DMDS were subtracted from the total gas yield, and all yields were calculated as a proportion of the DMDS-free feed (i.e. 99 wt% of the total feed).

During the FB-process, no pressure drop over the reactor column was observed (Supporting Information, Fig. S1). After terminating the process, letting the system cool down, and purging with nitrogen, the reactor was opened and the catalyst particles were poured out. The particles showed no sign of coking or fouling as they easily separated. The obtained product fractions resembled completely transparent organic phases and slightly yellow/greenish aqueous phases at the bottom (Supporting Information, Fig. S2).

2.4. Fractional distillation of hydrotreatment products

The aqueous phases from the FB-process, samples 6 through 11, were separated and the remaining organic phases were pooled. A fraction of the pooled product (187.81 g) was subjected to fractional distillation: A 500 mL round-bottomed flask was equipped with a Vigreux column, a Liebig condenser and a collection flask. A stirrer hotplate and an aluminum heat block (DrySyn®) were used for heating, and a high vacuum pump was connected via a 3-stage cooling trap using liquid N_2 as cooling media. Between the collection flask and the cooling trap a valve was mounted to enable emptying of the cooling trap without the need to depressurize the system. A fraction boiling below 177 °C was collected at atmospheric pressure and a second fraction in the atmospheric boiling point range 177–343 °C was then collected at reduced pressure. Using the estimated heat of vaporization, the boiling point at atmospheric pressure could be calculated and the distillation was terminated when the calculated atmospheric boiling point of 343 °C was obtained. At this point no more distillate could be collected and the residue in the distillation bulb was left as a third fraction (>343 °C).

2.5. Analytics

The products from the slurry-process and the FB-process were

analyzed by several techniques. Elemental composition (C, H, N, O and S) was analyzed by Elemental Microanalysis, United Kingdom. CHNS analyses were performed using the Dumas combustion method and O analyses using the Unterzaucher pyrolysis method. Carbonyl content was analyzed by potentiometric titration according to ASTM E3146-18a, and total acid number (TAN) according to ASTM D664. Boiling point distributions of the samples were analyzed by simulated distillation by GC according to ASTM D2887, or by thermogravimetric analysis (TGA) when GC-Simdist was not applicable due to high concentrations of oxygen. TGA was also used to evaluate the coking tendencies of some samples. TGA experiments were performed using a Mettler-Toledo instrument. Samples were prepared by accurately weighing 15–35 mg material into a 100 μL aluminum cup, which was then capped, and a small hole was punched into the lid using a cannula. The experiment set-up was the following: Ramp from 25 to 500 °C at 10 °C per minute, followed by an isothermal stage at 500 °C for 15 min. A continuous gas flow of nitrogen at 50 mL/min was applied throughout the measurement. The stability of the Heavy Product from the slurry-product was evaluated by measuring the kinematic viscosity (via a glass capillary tube) before and after being exposed to 80 °C for 24 h in a water bath.

NMR characterization experiments were performed on a 500 MHz Bruker AV1 spectrometer equipped with a 5 mm QNP probe head with *Z*-gradients operating at 25 °C. Samples for ^{1}H NMR were prepared by dissolving 40 μL oil in 600 μL $CDCl_3$ or DMSO-d_6 (FPBO only). Samples were analyzed with an experiment employing 60 s relaxation delay to ensure quantitative conditions. Spectra were referenced to residual $CHCl_3$ at 7.27 ppm or residual DMSO-d_5 at 2.50 pm. Samples for ^{13}C NMR were prepared by mixing 200 μL sample with 300 μL $CDCl_3$ or DMSO-d_6 (FPBO only). Samples were analyzed with an experiment designed for qualitative conditions only. Spectra were referenced to $CDCl_3$ at 77.16 ppm or DMSO-d_6 at 39.51 ppm. Samples for hydroxyl number determination using ^{31}P NMR were prepared by derivatizing approximately 50 mg oil with 2-Chloro-4,4,5,5-tetramethyl-1,3,2-dioxaphospholane (TMDP) in a solution of pyridine:$CDCl_3$ (1.6:1) in the presence of internal standard cyclohexanol and relaxation agent Cr(III)$(OAcAc)_3$. The samples were then analyzed using a ^{31}P experiment with inverse gated proton decoupling. Spectra were referenced to the signal from the internal standard at 144.9 ppm.

Aromatic content analyses were performed according to the method SS 12916:2019 using a Zorbax NH2 column (4.6 mm × 150 mm, 5 μm) from Agilent. The analyses were performed on a Thermo Dionex P680 or an UltiMate 3000 chromatograph equipped with a RefractoMax 520 refractive index (RI) detector. The columns were kept at 25 °C and the RI detector at 30 °C. Samples of approximately 0.1 mg/mL were prepared in heptane and those not fully dissolved were filtered prior to analysis. Heptane at 1 mL/min was used as eluent.

In addition to the above techniques, two-dimensional GC × GC–MS/FID was also used to characterize the liquid products. An Agilent 7890-5977 A, equipped with an oven, a flow splitter, a modulator, and a flame ionization detector was used for the analysis. The liquid products were separated by two columns, a mid-polar column (VF-1701MS, 30 m × 250 m × 0.25 m) and a non-polar column DB-5MS (1.2 m × 150 μm × 0.15 μm). The injection was done via an automatic liquid sampler into the GC injector at 280 °C. The oven temperature was initially kept at 40 °C for 1 min and then ramped up to 280 °C with a rate of 2 °C/min. The modulation time was set at 5 s for all samples and the flame ionization detector was set at 250 °C. The analysis was done using the GC image software for multidimensional chromatography. The product selectivity (%) was calculated based on the ratios of the individual component blob volumes to the total blob volume of the identified compounds in the liquid samples.

3. Results and discussion

3.1. Product properties

The slurry-process resulted in an oil product with a reduced oxygen concentration of 15 wt%, compared to 36 wt% of the dry FPBO (Table 2). Even though the oxygen concentration was still relatively high in the slurry-product, the oil product contained only 24.6 wt% of the non-water oxygen originally present in the FPBO but this remaining oxygen became concentrated in the reduced mass of oil product. This enrichment of course also applies to all oxygenated species as presented in Table 2. ^{31}P NMR shows that the amount of aliphatic alcohols and carboxylic acids are efficiently lowered by the slurry-process, while the phenol concentration was as high in the slurry-product as in the dry FPBO. This is not illogical, since phenols are known to have a relatively high resistance to hydrotreatment reactions and can also be formed by demethylation of methoxy groups during the slurry-process [28], in addition to the already mentioned concentration effect. Further hydroprocessing in the FB-process reduced the oxygen content to as low as 0.5 wt% and reduced the presence of hydroxyl groups to hardly detectable levels. The TAN and the carbonyl content were both halved by the slurry-process, and then removed to below detection limits in the FB-process.

^{1}H NMR data is a bit more difficult to interpret, with the high water

Table 2
Properties of the FPBO, slurry-product and FB-product. *As used in FB-upgrading, **Sample 11 from the FB-upgrading.

Elemental composition	Unit	FPBO (as received)	FPBO (dry)	Slurry-product*	FB-product**
C	wt%	46.1	58.6	72.5	85.4
H	wt%	6.8	5.6	9.4	13.4
N	wt%	0	–	0.06	< 0.05
S	wt%	0	–	< 0.1	< 0.1
O	wt%	47.1	35.8	15.0	0.5
Water Content	wt%	21.2	0.0	0.0	0.0
^{1}H NMR					
Alkanes	mol-%	42.3[1]	–	77.8	96.0
Alcohol/Ether (CH_x-O)	mol-%	33.0	–	7.8	0.0
Alkene	mol-%	10.1	–	4.5	0.0
Aromatics	mol-%	13.4	–	9.9	4.0
COOH/ Aldehydes	mol-%	1.3	–	0.01	0.0
^{31}P NMR					
Aliphatic OH	mmol/g	4.0	5.1	0.8	0
Phenol OH	mmol/g	2.3	3.0	2.9	0.004
COOH	mmol/g	0.8	1.0	0.5	0.001
Total OH	mmol/g	7.1	9.1	4.2	0.005
Carbonyls	mmol/g	4.2	5.3	2.4	Not detected
Total Acid Number	mmol/g	1.2	1.5	0.7	Not detected
Aromatic content by HPLC-RI					
Mono aromatics	wt%	Not measured	Not measured	4	29.0
Di aromatics	wt%			3	2.5
Tri and higher aromatics	wt%			0.4	0.0
Total aromatics	wt%			7.4	31.5

[1] The proton NMR data for FBPO is made less precise by the high water content in the sample.

content of the FPBO making accurate integration difficult. However, the reduction in oxygen over the two process steps agrees well with a stepwise reduction in aliphatic alcohols, which cannot be detected in the FB-product. Alkenes are also reduced in a stepwise manner and are not detected in the FB-product, while the aliphatic hydrocarbon content is gradually increased throughout the two process steps. In the ^{1}H NMR data, the aromatic content seems to decrease through the processing, although according to the aromatics analysis the aromatic content is dramatically increased in the FB-process. This discrepancy can be explained by the fact that the aromatic analysis yields results in wt% of actual aromatic compounds, while ^{1}H NMR yields results in mol % based on the position of all protons. For example, substituted aromatic hydrocarbons will be evaluated as aromatic compounds according to the aromatics analysis, while the proton NMR data will show signals from the aromatic protons as well as signals from the aliphatic substituents, thus skewing the result towards a higher aliphatic content and lower aromatic content. The H/C atomic ratio of 1.88 for the FB-product agrees well with a composition of primarily alkanes and substituted mono-aromatics.

The tabulated data is well mirrored in the ^{13}C spectra (Fig. 3), which were collected qualitatively and the results are therefore not tabulated. However, it can be seen that the slurry-process is very efficient in lowering the concentration of aldehydes, ketones, carboxylic acids and esters (which can be seen in the 215–163 ppm range of the spectra), as well as carbohydrates (110–84 ppm), while the FB-process further removes all oxygenates to yield a hydrocarbon product. It should be noted that the chemical shifts of alkenes overlaps with those of the aromatics, so removal of alkenes is best monitored by ^{1}H NMR.

A reactivity ranking of oxygenated groups under hydrotreatment conditions has been proposed elsewhere [15], suggesting that the reactivity decreases in the order: carbonyls > aliphatic ethers > aliphatic alcohols > carboxylic groups > phenolic ethers > phenols. In this study, the conversion of the different oxygenates in the slurry-process, according to ^{31}P NMR and carbonyl titration, decreased in the order: aliphatic alcohols (93%) > Carbonyls (78%) = COOH (78%) > Phenols (49%). These numbers were obtained by comparing the number of moles present in the oil products obtained from one kg FPBO to the number of moles originally present in one kg FPBO (the FB-process resulted in near complete conversion for all compound groups and a similar comparison is not relevant in that case). Phenolics clearly exhibit the lowest reactivity to hydrodeoxygenation, which agrees well with the proposed scale. Aside from that, alcohols actually showed the highest conversion, and not carbonyls as suggested by the reactivity scale. As carbonyls have been suggested to have the highest reactivity under hydrotreatment conditions [15,29], their incomplete (and similar to carboxylic acids) conversion is a bit surprising.

The progression of the oil product towards a more deoxygenated and hydrogenated state throughout the process steps is shown in Fig. 4, with the results of Dimitriadis et al. [25], who also upgraded FPBO in a slurry-process followed by a FB-process, included as a comparison. The FPBO used by Dimitriadis et al. had a lower O/C and a higher H/C atomic ratio to begin with, which might explain the very similar properties of the slurry-product as in this study, despite the lower reaction severity used in the study by Dimitriadis et al. (350 °C and a LHSV of 1 h^{-1}, but on the other hand a higher pressure of 150 bars). Fixed bed upgrading of the stabilized FPBO (at 330 °C, 69 bars, 1 h^{-1} LHSV and 840 L/L gas to liquid feed ratio) by Dimitriadis et al. resulted in an oil product with higher oxygen concentration (3.1 wt%) and a lower H/C atomic ratio (1.6) than in this study (0.5 wt% and 1.88). The more severe conditions of the FB-reaction in this study (380 °C, 100 bars, 0.5 h^{-1} LHSV) may explain the more complete deoxygenation and hydrogenation obtained in this work. However, the reduction of the reaction temperature to 340 °C towards the end of the FB-upgrading of this work resulted in only a minor increase in the oxygen concentration of the product to 0.7 wt% (Table 3) and the temperature may therefore not be primarily responsible for the differences.

3.2. Stability of the slurry-product

Carbonyls (aldehydes and ketones) are known to contribute to the instability of FPBO due to their tendency towards oligomerization reactions and condensation reactions with, for example, phenolic compounds [30,31]. Due to this, reducing the amount of carbonyls has been a focus in other studies aiming to stabilize FPBO. For instance Zacher et al. [14] described a goal of reducing the carbonyl concentration to <2.5 mmol/g in the stabilized bio-oil but observed even better results at <1.5 mmol/g. In this study, the carbonyl concentration decreased from 4.2 mmol/g in the as received FPBO to 2.4 mmol/g in the slurry-product. An actual increase in stability of the slurry-product is evident from the change in viscosity after an accelerated aging test of the untreated FPBO and the slurry-product (only the Heavy Product in this case) for 24 h at 80 °C. For untreated FPBO the viscosity increased from 36.4 to 46.1 mm^2/s while the slurry-product showed nearly identical results before and after aging (12.2 and 12.0 mm^2/s, respectively). Furthermore, the slurry-product (as used in the FB-process) showed a residue of 1.4 wt% after heating to 500 °C in an inert atmosphere in a thermogravimetric analyzer (TGA). This is drastically lower than that typically observed for FPBO, where the amount of residue can be in the range of 20 wt% due to coke formation [32]. In our previous work, where FPBO was stabilized at a lower reaction temperature (350 °C), the micro Conradson Carbon Residue (which also involves heating a sample to 500 °C in an inert atmosphere and is normally used as an indicator for coking tendencies) decreased from 24.5 wt% in the FPBO to 12.5 wt% in the stabilized FPBO, even though the carbonyl concentration of the stabilized FPBO in that study was lower (1.5 mmol/g) than in the present work [25]. Although the TGA residue might not be directly comparable to the micro Conradson Carbon Residue, it appears that the carbonyl concentration in itself is not a good indicator of the stability (or at least the coking tendency) of the stabilized FPBO. Furthermore, the much higher coking tendency of the stabilized FPBO used in our previous study [25] might have been responsible for the more rapid catalyst deactivation observed (already after the first 24 h), which suggests that TGA residue (or Conradsson Carbon Residue) might be a good indicator for the performance of a partly deoxygenated FPBO in an FB-process. The lower coking tendency of the slurry-product obtained in this study could be related to the much higher reaction temperature used (410 vs. 350 °C), although differences in catalyst and catalyst loading, FPBO properties etc. cannot be excluded. Another study on the stabilization of FPBO, using different catalysts, has shown TGA residue levels of 3.2–5.0 wt% after reaction at 200 °C and 1.2–1.5 wt% after reaction at 350 °C [33]. With reported oxygen concentrations of 12–15 wt% after using the higher temperature, both the TGA residues and oxygen concentrations of their oil products agree very well with the results in this study.

3.3. Effect of reduced temperature in the FB-process

The properties of four samples collected at different times from the FB-process are shown in Table 3. As the temperature in the FB-reactor was decreased to 340 °C towards the end of the FB-processing (Sample 12) some differences were observed in the product properties. The oxygen concentration increased slightly to 0.7 wt% and this increase was also reflected in the ^{1}H NMR data which showed levels of alcohol/ether, and in the ^{31}P NMR data that showed increased levels of phenols. Some signals from alkenes could also be observed in the ^{1}H NMR results, which was not the case at the higher process temperature. The lower temperature also seemed to reduce the proportion of aromatics in the product as can be confirmed by the aromatics analysis using HPLC-RI. The properties of Sample 13, which was collected near the end of the FB-processing, when the reaction temperature had been increased to 380 °C again, corresponded very well with those of the samples collected at same reaction temperature in an earlier stage (Sample 4 and 11), which suggests no, or very limited, reduction in catalytic activity.

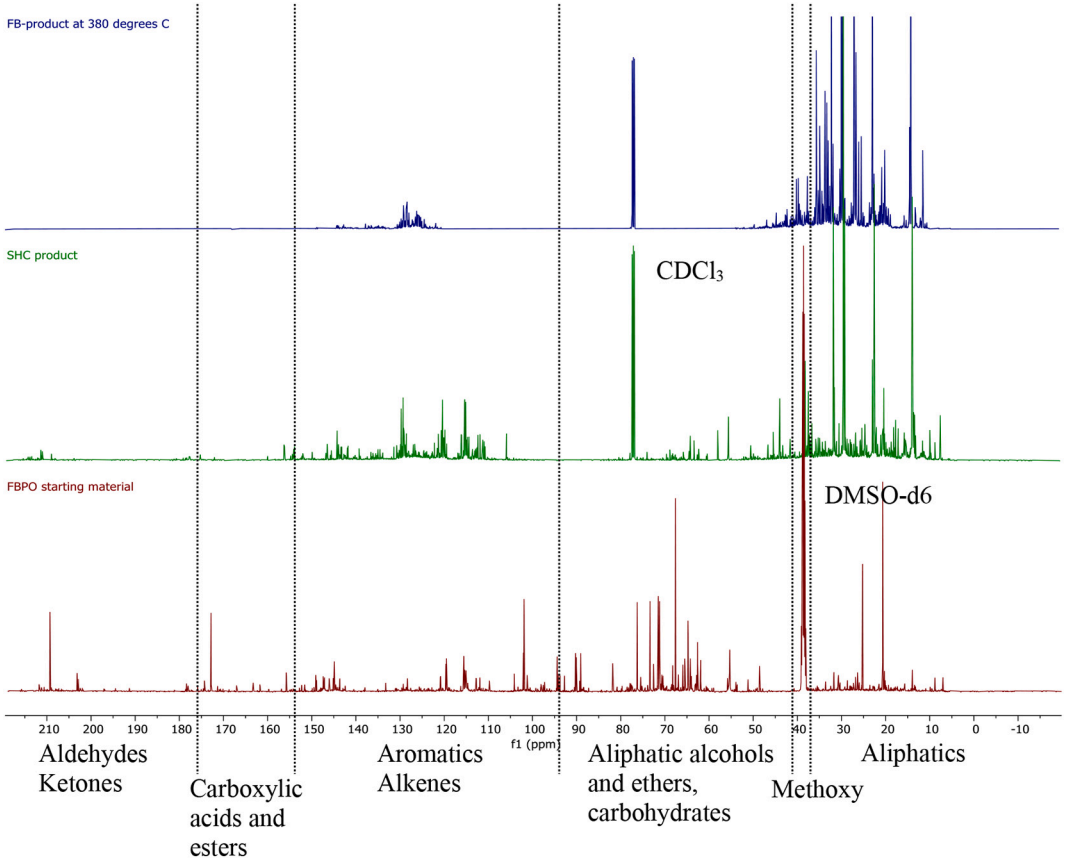

Fig. 3. ^{13}C NMR spectra of FBPO (bottom), slurry-product (middle) and FB-product (top).

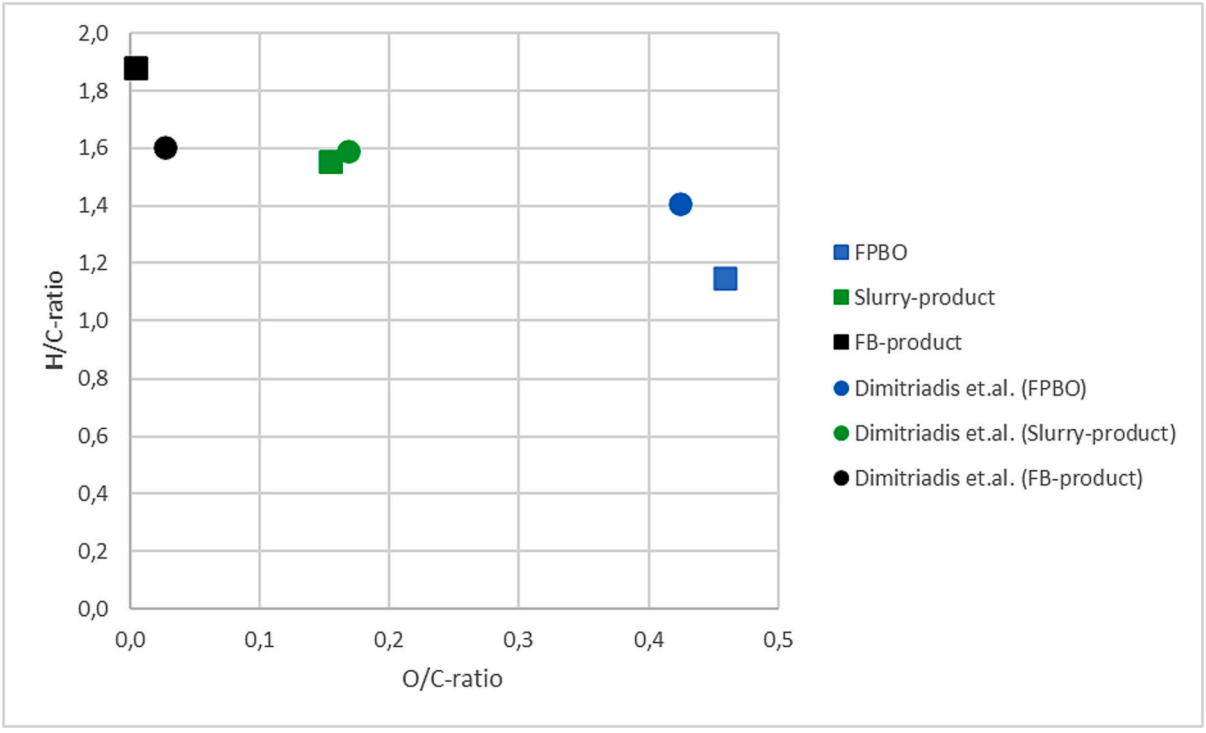

Fig. 4. Van Krevelen diagram showing the atomic ratios of O/C and H/C for the FPBO (dry basis) and the two oil products (squares). The results of Dimitriadis et al. [25] is shown for comparison (circles).

Table 3
Selected analytical properties of samples 4, 11, 12, and 13 from the FB-process. Sample 12 was collected at a lower reaction temperature (340 °C) than the other three (380 °C).

	Unit	Sample 4	Sample 11	Sample 12	Sample 13
Reactor temperature	(°C)	380	380	340	380
Elemental Composition					
C	wt%	84.9	85.4	85.6	86.1
H	wt%	13.4	13.4	13.7	13.3
N	wt%	Not detected			
S	wt%	Not detected			
O	wt%	0.4	0.5	0.7	0.5
^{1}H NMR					
Alkanes	mol-%	96.4	96.0	97.4	95.8
Alcohol/Ether	mol-%	0.0	0.0	0.1	0.0
Alkene	mol-%	0.0	0.0	0.1	0.0
Aromatics	mol-%	3.6	4.0	2.5	4.2
COOH/Aldehydes/ Phenol	mol-%	Not detected			
^{31}P NMR					
Aliphatic OH	mmol/ g	Not detected			
Phenol OH	mmol/ g	0.0	0.004	0.1	0.0
COOH	mmol/ g	0.0	0.001	0.00	0.0
Total OH	mmol/ g	0.0	0.005	0.1	0.0
Carbonyls	mmol/ g	Not detected			
Total Acid Number	mmol/ g	Not detected			
Aromatic content by HPLC-RI					
Mono aromatics	wt%	29	29	19	27
Di aromatics	wt%	1	2	2	4
Tri and higher aromatics	wt%	Not detected			
Total aromatics	wt%	30	31	21	31

3.4. Properties of distillation fractions

The FB-product was, according to GC-Simdist, distributed roughly as 46 wt% boiling below 177 °C, 48 wt% boiling between 177 and 343 °C, and the remaining mass (6 wt%) boiling above 343 °C (Fig. 5). The two former ranges correspond approximately to gasoline and diesel boiling point ranges, suggesting that a majority of the components in the FB-product are in a range suitable for the production of these fuels. According to TGA, the slurry-product (as used in the FB-process) had a significantly higher boiling point range with only around 17 wt% boiling at a temperature below 177 °C. The GC-Simdist data of the FB-products (Fig. 5) show a horizontal shape around 287 °C, which corresponds to the boiling point of hexadecane. This implies that some hexadecane, which was used as a starting oil in the slurry-process, was recovered to both the slurry-product and the FB-product even though a hexadecane phase was separated from the Heavy Product. The two Heavy Products obtained from the slurry-process (early and late) were at first analyzed separately by several techniques but showed relatively similar results (Supporting Information, Table S1) and were therefore mixed for the FB-processing (as this would enable longer time on stream). Nevertheless, approximately 6 wt% of the FB-product consisted of hexadecane.

The FB-product fractions obtained at 380 °C were pooled and subjected to fractional distillation with fractions collected up to 177 °C, at 177–343 °C and a residue above 343 °C. The isolated amount of the faction below 177 °C was 37 wt% of the FB-product and the fraction collected at 177–343 °C was 51 wt% of the FB-product, corresponding relatively well to the amounts predicted by GC-Simdist. The amount of distillation residue (the >343 °C fraction) corresponded to 3.7 wt% of the total distilled mass and had a brown color, in contrast to the lack of color of the starting material and the other distillation fractions. The total mass recovery from the distillation, including the cold trap fraction of 2.1 wt% was 94.3 wt%. The analytical properties of the fractions are given in Table 4. The lighter fraction displayed the lowest oxygen concentration (0.28 wt%), highest H/C atomic ratio (1.96), and lowest aromatics signal according to ^{1}H NMR (2.6 mol-%). In contrast, the fraction boiling above 343 °C showed the lowest H/C atomic ratio (1.52) and highest aromatics signal according to ^{1}H NMR (7.9 mol-%). In a recent study, the distillation residue (> 360 °C) obtained from hydroprocessed FPBO (i.e. a fraction similar to the >343 °C fraction obtained in this study) was co-processed with vacuum gas oil in a fixed bed hydrocracker (420 °C, 160 bars), showing that this boiling point fraction can be successfully further upgraded [34].

3.4.1. GC X GC-MS/FID

The GC × GC–MS/FID analysis showed a significant presence of oxygenated compounds in the slurry-product (Fig. 6a) but in the FB-product hardly any such signals were detected (Fig. 6b). As indicated in the 2D GC × GC–MS/FID spectra, the slurry-product contained a wide spectrum of products, including paraffinic-derived compounds, deoxygenated aromatics, phenolics, furanics, ketones, aldehydes, carboxylic acids, cycloalkane-derived compounds, dimers, and polyaromatics. This complex and still highly oxygenated structure of the slurry-product agrees well with the results previously discussed (Table 2 and Fig. 3). In contrast, the FB-product consisted of mainly paraffinic-derived compounds, cycloalkanes, and aromatics, as shown in the GC × GC spectra (Fig. 7b), with no oxygenated species being detected. This also agrees well with previously presented results. As some hexadecane was recovered from the starting oil in the slurry-process, peaks corresponding to this compound were not integrated and do not represent part of the "paraffinic derived compounds" in Fig. 7. Noteworthy is that the two distillation fractions (< 177 °C and 177–343 °C) both showed very high levels of cycloalkanes according to 2D GC × GCMS/FID (49% and 37% at the lower and higher boiling point range, respectively), something that cannot be determined by other techniques previously discussed.

For the <177 °C fraction, the results of the aromatics determination by HPLC-RI and by 2D GC x GC–MS/FID agree very well (ca 10% mono-aromatics and no di-aromatics or naphthalene-derived compounds are expected). However, for the 177–343 °C fraction the results differ significantly, with HPLC-RI resulting in 46 wt% mono-aromatics and 9 wt% di-aromatics, while GC results show 9% aromatics and 17% naphthalene-derived compounds. A major difference exists between how the two methods categorized the compounds; HPLC-RI will consider naphthalene as di-aromatic but if one of the aromatic rings is saturated it will be considered a mono-aromatic, while the GC x GC library will categorize both these compounds as "naphthalene-derived". This suggests that a large part of the mono aromatics detected by HPLC-RI are indeed derived from naphthalene but one of the aromatic rings is saturated. Furthermore, it is possible that heavier substituted naphthalene-derived compounds do not reach the detector in the 2D GC x GC–MS/FID analysis (highest boiling point observed was 312 °C), thus resulting in an underestimation of this fraction. Nevertheless, the products show a predominance of cyclic compounds (aromatic and aliphatic), which has also been observed in hydrotreated pyrolysis oils by others [10,35].

3.5. Spent FB-catalyst

The elemental composition of the spent catalyst from the FB-process was analyzed and showed some presence of carbon residue (4.9–12.4 wt %) but no clear trend versus the distance from the reactor inlet could be

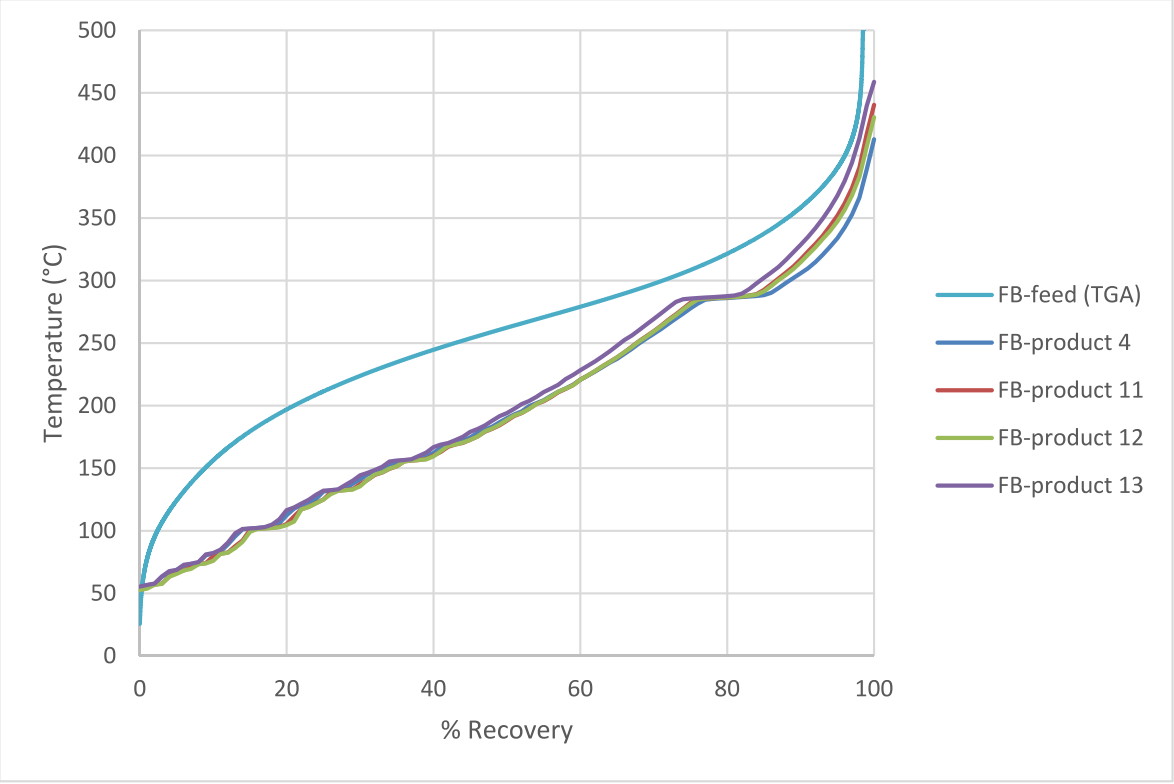

Fig. 5. Boiling point distribution of FB-products (GC-Simdist) and the slurry-product used as feed for the FB-process (TGA). The horizontal shape of the curve around 287 °C for the FB-products is due to some of the hexadecane used as starting oil in the slurry-process being recovered in the final product.

Table 4
Properties of the distillation fractions of the FB-product.

	Unit	< 177 °C	177–343 °C	> 343 °C
Distillation yield	wt%	37.4	51.3	3.7
Elemental Composition				
H/C	mol%/mol %	1.96	1.77	1.52
O	wt%	0.28	0.46	0.32
^{1}H NMR				
Alkanes	mol-%	97.4	94.7	91.6
Alcohol/Ether (CH_x-O)	mol-%	0.02	0.05	0.54
Alkene	mol-%	0.00	0.00	0.01
Aromatics	mol-%	2.6	5.2	7.9
COOH/Aldehydes	mol-%	0.0	0.0	0.0
Aromatic content by HPLC-RI				
Mono aromatics	wt%	10	46	Not
Di aromatics	wt%	0.1	2	analyzed
Tri and higher aromatics	wt%	0	0	
Total aromatics	wt%	10.1	48	

observed, except for less carbon residue at the very end of the catalyst bed (Supporting Information, Fig. S3). These results suggest that some organic residue may accumulate on the catalyst, but the H/C atomic ratios were relatively high (1.4–2.0), which indicates that the residue is not very polyaromatic in its structure, something that is normally observed in coke from hydroprocessing catalysts [13,36,37]. Hence, the carbon residue does not necessarily resemble typical coke. Another possible source of carbonaceous residue is solids already present in the slurry-product, which was not successfully removed by the filtration at 10–20 μm. The centrifugated Heavy Slurry-product contained approximately 0.6 wt% acetone-insoluble solids (1.2 wt% before centrifugation) and a significant part of these particles were likely smaller than 10 μm since they were not removed by centrifugation. In terms of quantity, it was estimated that 0.7 wt% of the carbon passed through the FB-reactor could be accounted for in the carbonaceous deposits on the catalyst, although it cannot be concluded from this study if this material was actually produced in the process or simply accumulations of already solid particles present in the feed.

3.6. Yields from FPBO

The mass balance closure was 99.6% for the slurry-process and 96.8% for the FB-process (operated at 380 °C) and the corresponding carbon balances were 91.3% and 86.0%, respectively (calculated with elemental analysis results normalized to 100%). The mass balance for the slurry-process was calculated towards the end of the experiment, when the process was most stable and carbon balance for the FB-process corresponds to the average of six individual balances corresponding to the periods at which samples 6–11 were produced (individual balances are presented in Supporting Information, Table S2).

The mass- and carbon balances presented in Figs. 8 and 9 have been normalized to 100%.[1] Since the mass balance closures were relatively high, this normalization introduced small corrections. The carbon balance closures were on the lower end but the reasons behind this are hard to elaborate, especially since the mass balances were considerably higher. One source of carbon loss in the FB-process is the accumulation

[1] The mass balance reported here is the total mass of liquid and gaseous product (not including H_2) in relation to feed mass. Due to H_2 addition the mass balances calculated in this way should logically be higher than 100% but normalization has still been done to 100%, not to introduce any unwarranted overestimations. The carbon balances, on the other hand, should ideally be exactly 100%.

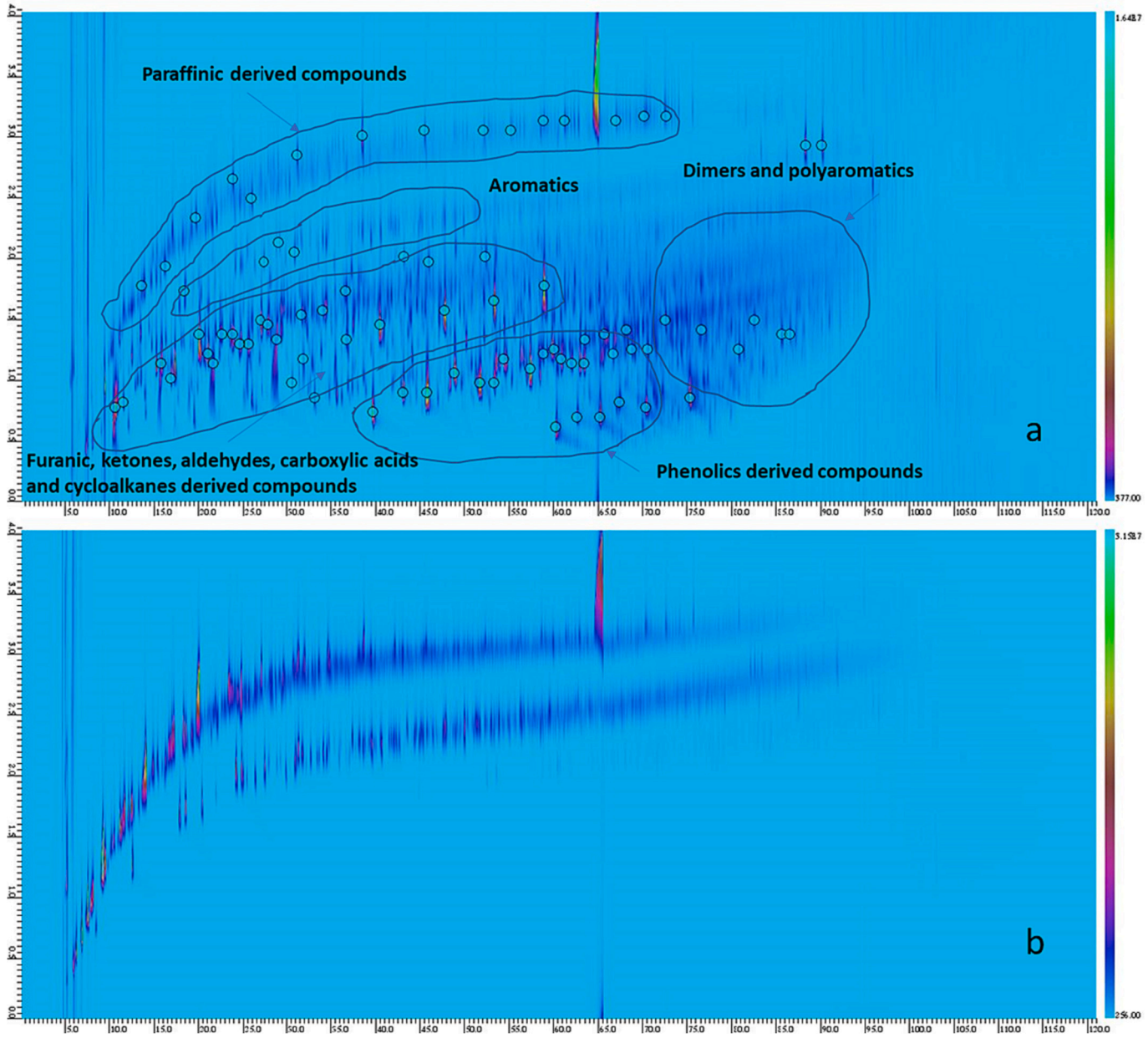

Fig. 6. GCxGC-MS/FID spectra of the slurry-product as used in the FB-upgrading (a) and sample 11 of the FB-product (b). The products were classified into different groups as indicated in figure (a).

of material in the catalyst bed but, as already noted, this carbon mass was approximated to only 0.7 wt% of the total mass of carbon fed to the process and therefore only seems to compensate for a small part of the deviation in the carbon balance.

The yield of acetone-insoluble solids in the slurry-process was 0.3 wt %, with a large part of this being catalyst, and is not considered in the mass balance. It is clear that significant coke formation did not take place, which is in line with previous studies using slurry-hydroprocessing of FPBO both with co-feed [20,21] and with only FPBO [26]. It is generally considered that to limit coke formation from FPBO when hydroprocessing in fixed bed reactors a stabilization reaction step at low temperature (100–300 °C) to deoxygenate the most reactive species is first required, although complete elimination of problems associated with coke formation is difficult even with this strategy [7]. The reasoning is that this stabilization must occur at temperatures low enough so that no (or limited) coke-forming polymerization reactions take place, whereas subjecting the FPBO to high temperatures (> 375 °C) without prior stabilizaiton leads to severe coke formation [38]. The strategy of stabilizing the FPBO at low temperature is very different from the slurry-process used in this study, where the temperature was very quickly increased to 410 °C without any chance for stabilization at low temperatures. It seems the slurry-process works well in suppressing the coke formation but it is not well understood why this is the case. One possible explanation is that the turbulent environment in a slurry-reactor (in contrast to fixed bed reactors) results in rapid contact between feed and catalyst (catalyst is also already suspended in the feed that enters the reactor), which favors an effective suppression of coke-forming reactions. However, experiments in stirred batch reactors (where the environment is also very turbulent) typically generate significant amounts of coke as well [13], so this cannot be the sole explanation. Furthermore, in our previous study we found superior results when co-feeding FPBO with fossil feedstock to a hot reactor compared to reacting a similar mixture in a semi-batch setup [20]. The continuous feeding results in both a very rapid increase to the reaction

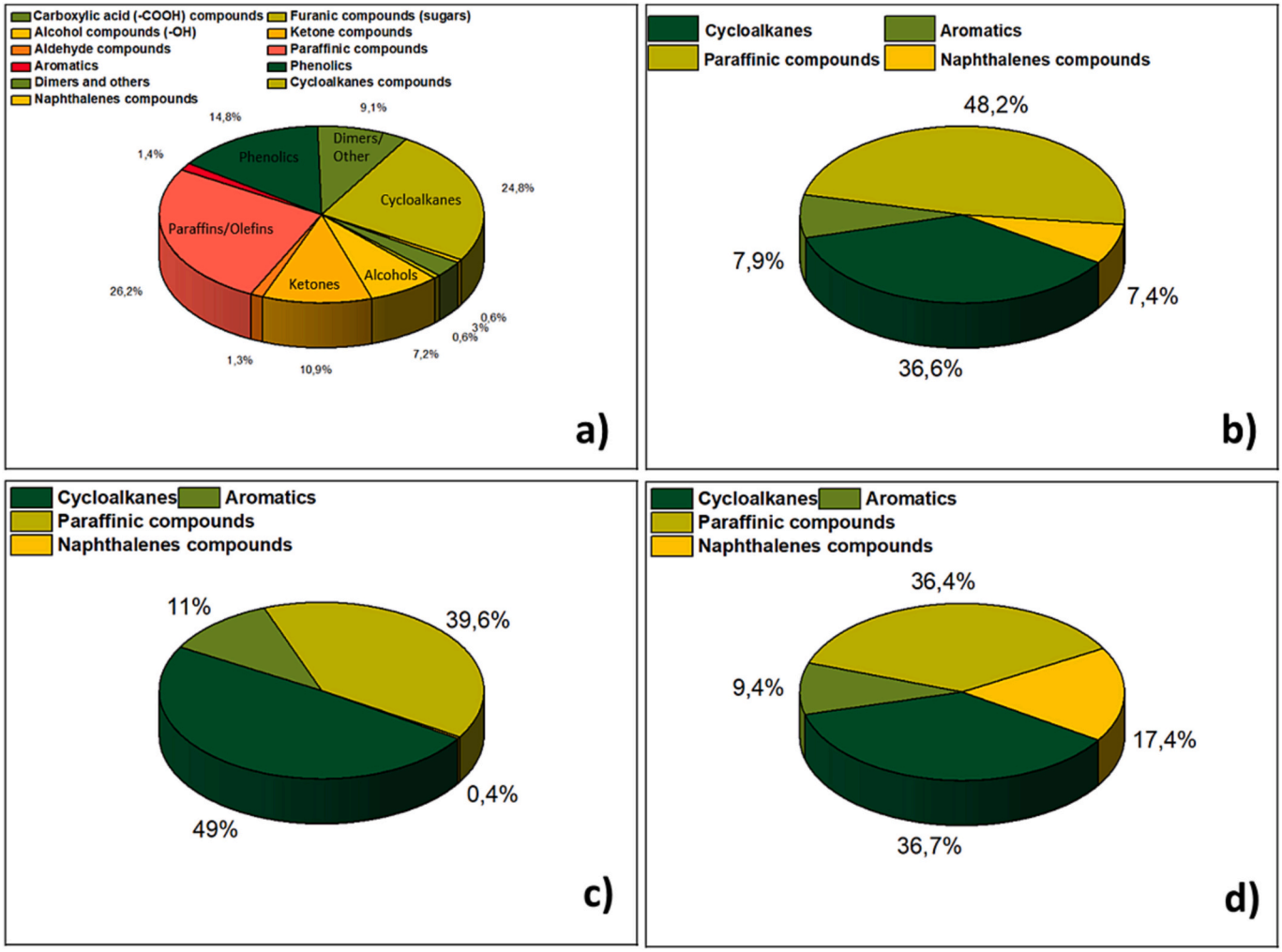

Fig. 7. Distribution of compound classes as FID area-% according to GCxGC-MS/FID a) slurry-product, b) FB-product, c) Distillation fraction <177 °C of FB-product, d) Distillation fraction 177–343 °C of FB-product.

temperature but also a quick mixing of fresh feed with the reactor contents. Reduced coke formation has been observed by mixing FPBO with different solvents before processing [13], and it is possible that a similar coke-suppressing effect can be achieved by the reactor contents (which should already be free of the most reactive species). Nevertheless, coke formation from FPBO is a complex phenomenon that is not fully understood and there may be several interacting factors affecting the outcome.

In the slurry-process there is a significant loss of both mass and carbon to the water product and to gas (Figs. 8 and 9). Among the gas products, quite similar quantities of carbon oxides (7.1 wt%) and gaseous hydrocarbons (6.5 wt%) were produced. However, CO_2 constituted a three times greater mass yield than CO and was the dominating gaseous species (5.4 wt%), followed by CH_4 (2.8 wt%). A high ratio of CO_2 to CO is preferred, as CO_2 involves removal of twice as many oxygen atoms per carbon atom, which in turn contributes to an increased carbon recovery to the liquid products at a similar deoxygenation level. The carbon contents in the water products produced in the slurry-process were relatively high; 10.7 wt% in the water product collected from the LP-LT separator and 15.4 wt% in the water product separated gravimetrically from the Heavy Oil Product. The FB-process produced additional water product from the remaining oxygen, but this contained only 0.5–3.1 wt% carbon and almost 97 wt% of the carbon in the feed was recovered in the oil product. Combining the two processes, the yield of oil product from the FPBO was 28.7 wt% and the recovery of carbon was 67.7 wt%. The H_2 consumption was 42.7 g per kg dry FPBO in the slurry-process and 20.3 g per kg feed in the FB-process, which results in a total H_2 consumption for both steps of 52.6 g per kg processed dry FPBO (or 140 g H_2 per kg produced deoxygenated oil product).

It should be noted that the mass balance for the slurry-process was calculated towards the end of the experiment, when the Heavy Product did not contain any of the hexadecane starting oil. Hence, the mass- and carbon balances reported are not affected by the recovery of hexadecane to the Heavy Product during the earlier parts of the experiment. For the FB-process, the effect of the presence of hexadecane in the slurry-product used in the FB-process was very small for the carbon balance because the carbon recovery was very high for both the hexadecane and the non-hexadecane part of the feed. For the mass balance the presence of hexadecane led to a very slight overestimation of the oil product yield (the hexadecane presumably had a higher recovery in the oil product than the remainder of the feed).

3.7. Comparison with literature data

The H_2 consumption and carbon recovery throughout the pyrolysis and hydroprocessing steps is tabulated in Table 5, along with comparison of data from the literature (calculated based on data from the respective study). In this study, the mass yield of pyrolysis oil from biomass is not known as the pyrolysis oil used was of a commercial type

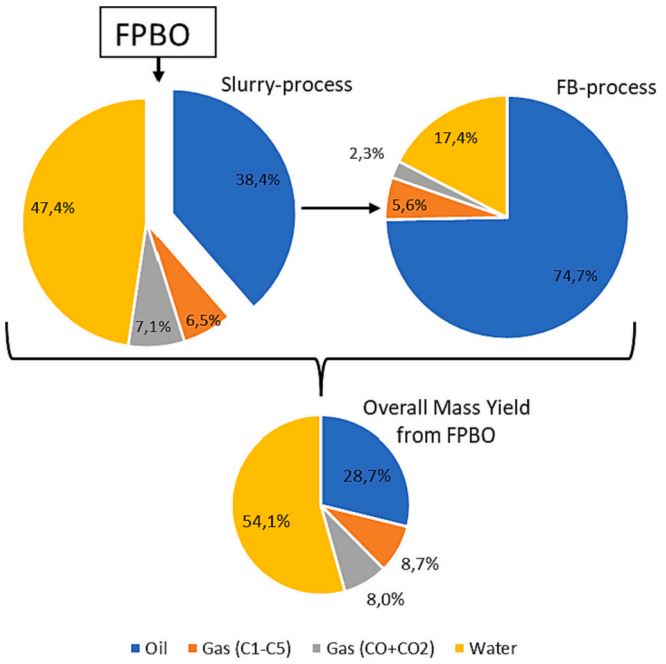

Fig. 8. Normalized mass balances of the two process steps and the overall yields from FPBO by combining both hydroprocessing steps.

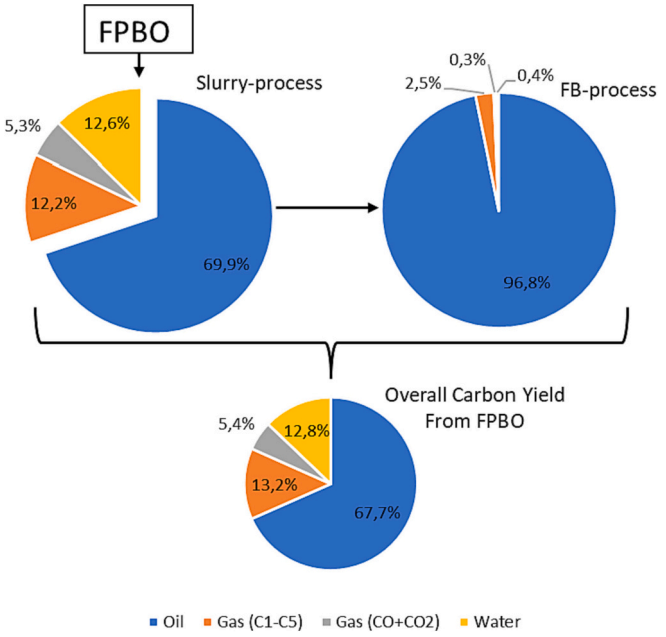

Fig. 9. Normalized carbon balances of the two process steps and the overall yields from FPBO by combining both hydroprocessing steps.

and not produced in the study. For the sake of discussion and comparison of the whole chain of process steps from pyrolysis to hydroprocessing, a carbon concentration of 50 wt% in dry biomass and a mass yield to FPBO of 60 wt% have been assumed, which are typical values for low-ash feedstocks such as pine wood [10,39]. The three studies used for comparison in Table 5 are briefly described here:

- In the study performed by Dimitriadis et al., a slurry-process was used to stabilize the FPBO obtained from wheat straw before upgrading in a (1-stage) FB-process [25], similarly as in this work. Although the slurry-process did improve the properties of the FPBO and provided a stabilized FPBO for further processing in the fixed-bed process, plugging issues were present and a decline in product properties was observed already after the first 24 h (and subsequently became worse even though the process could be maintained for up to 8 days of feeding). Data in Table 5 is calculated based on"RUN 7, DOS 1″.
- Catalyst deactivation (although no plugging problems during the 60 h processing time), was also observed by Elliot et al. when upgrading FPBO from red oak in a 2-stage FB-process, with the first (low-temperature) stage was intended to stabilize the bio-oil [40]. Data in Table 5 is calculated based on the "Unfiltered Oak" case, which showed overall the best yield among the cases studied.
- Agblevor et al. performed catalytic pyrolysis of pinyon juniper with red mud as a catalyst [41]. The catalytic pyrolysis oil was then successfully hydrotreated in a 1-stage FB-process (no low-temp stabilization step) for over 300 h without any significant catalyst deactivation or coke formation.

Table 5
Mass recovery, Carbon recovery, and H_2 consumption throughout the pyrolysis and hydrodeoxygenation stages. The oxygen content for each product (wt% on wet basis) is indicated in brackets next to the mass recovery of each product. * Assumed mass recovery of the pyrolysis process.

		Pyrolysis	Slurry-process	FB-process	Overall
Current study	Mass Recovery	60%* (36% O)	38% (15% O)	75% (0.5% O)	17%
	Carbon Recovery	56%	70%	97%	38%
	H_2 Consumption	–	34 (g/kg wet feed)	20 (g/kg wet feed)	140 (g/kg oil product)
Dimitriadis et al. [25]	Mass Recovery	42% (33% O)	57% (16% O)	81% (3% O)	19%
	Carbon Recovery	46%	82%	96%	36%
	H_2 Consumption	–	20 (g/kg wet feed)	29 (g/kg wet feed)	80 (g/kg oil product)
Elliot et al. [40]	Mass Recovery	69% (42% O)	–	47% (0.5% O)	32%
	Carbon Recovery	58%	–	78%	46%
	H_2 Consumption	–	–	38 (g/kg wet feed)	100 (g/kg oil product)
Agblevor et al. [41]	Mass Recovery	30% (19% O)	–	72% (1% O)	21%
	Carbon Recovery	41%	–	92%	37%
	H_2 Consumption	–	–	71 (g/kg wet feed)	100 (g/kg oil product)

No plugging problems or deterioration of the catalyst activity was observed in the present work during the 58 h processing time. These results are promising but longer studies are of course needed to study the stability of the process over time. Calculating with the assumed yield of FPBO from biomass, a significant loss of carbon (44%) is associated with the pyrolysis process in this study, which can be compared to the results of Dimitriadis et al. (54%) and Elliot et al. (42%). Noteworthy is that a higher ash content of the biomass is correlated with reduced yields of FPBO [39], and the relatively high ash content of the straw used by Dimitriadis et al. likely contributes to a comparatively low carbon recovery to the FPBO. The mass yield of catalytic pyrolysis oil in the process used by Agblevor et al. was low (30 wt%) compared to FPBO yields in the non-catalytic fast pyrolysis processes (42–68 wt%) and, as a result, the carbon recovery to the catalytic pyrolysis oil was also

comparatively low (41 wt%). However, the oxygen content of the catalytic pyrolysis oil was relatively low (19 wt%) and the hydroprocessing step provided a very high carbon recovery (92 wt%) compared to hydroprocessing (all steps included) of FPBO (66–78 wt%). This brings the overall carbon recovery from biomass via the catalytic pyrolysis route (37%) to the same range as the fast pyrolysis cases (36–46%). In fact, of the four cases, only the results from Elliot et al. stand out with 46% carbon recovery, while the other three are found to lie in a very narrow range of 36–38%. It should be noted that the composition of the final product differs between the different process concepts, as does the properties of the original biomass, and it is likely that such factors could explain some of the observed differences.

The hydrogen consumptions are in the range 80–140 g per kg produced deoxygenated oil product (last column of Table 5). The trends in the table suggest that if the H_2 consumption (per kg feed) is high at a stage where there is a large mass of feed being processed, this will result in an overall high consumption. A good example of this is the case with processing of catalytic pyrolysis oil [41], which did consume very large amounts of H_2 (71 g per kg feed) compared to any other individual process step. However, due to the low mass yield of catalytic pyrolysis oil from biomass (30 wt%), this left a relatively low mass of pyrolysis oil to process (i.e. only 300 g per kg starting biomass), resulting in a modest overall H_2 consumption. In the current study, the first hydroprocessing step had a much lower H_2 consumption of 34 g/kg feed than for the catalytic pyrolysis oil but due to the larger mass of pyrolysis oil being processed (600 g for each kg biomass), this contributed to an overall higher H_2 consumption.

The carbon recovery in the slurry-process (70%) was lower than in our previous study using a slurry-process to stabilize FPBO (82%) [25]. There seems to be three factors that contribute to a lower carbon recovery in this study: 1) nearly twice as high gas yield (nearly all of this excess is coming from gaseous hydrocarbons as the yield of carbon oxides show very small differences), 2) higher water phase yield, and 3) about twice as high carbon concentration in the water phase. It was expected that the higher temperature used in this study would lead to higher gas formation, and possibly also to a higher water phase yield. However, the reason for the higher carbon concentration in the water phase is not well understood. One possibility is that the higher reactor temperature and gas flow, and lower pressure, used in this study contributes to evaporation of light oxygenates from the reactor, before they have time to be sufficiently deoxygenated. However, this has not been confirmed. The organic compounds found in the water products are likely partly deoxygenated and, more or less, water-soluble species that become distributed between the oil- and water phases (in the Heavy Product tank or in the LP-LT separator) based on solubility properties. An optimized separation system in the slurry-process could likely reduce the loss of carbon to the water products, which would increase the oil product yield and carbon recovery to the oil product. Although a water fraction with as high as 15 wt% carbon is not useless, and steps could be taken to valorize these organic compounds. A study using mild stabilization (200 °C) of FPBO has been shown to result in even higher recoveries of carbon to the water phase, in the range 40–61 wt%, and has briefly discussed the possible valorization of this fraction [42]. In contrast, a 2-stage FB-process, which does not produce any intermediate water products at low deoxygenation levels, can result in carbon concentrations as low as 0.6 wt% in the water phase and, hence, a very low carbon loss to the water product [9]. Consequently, these observations suggest that the lower the level of deoxygenation at which an intermediate water phase is withdrawn from the deoxygenation process, the higher will be the "loss" of carbon to this water phase. Therefore, using a single hydroprocessing step, such as in the case for Elliot et al. [40] and Agblevor et al. [41] in Table 5, will of course contribute to higher carbon recoveries compared to using separated hydroprocessing stages.

Based on Table 5, there are no clear distinctions between the different hydroprocessing techniques, as the processes investigated in the respective studies do not clearly outperform each other in terms of carbon recovery or H_2 consumption. This suggests that, in the end, it likely comes down to what is the most robust and economically viable method for production of hydrocarbons through pyrolysis and hydroprocessing of lignocellulosic biomass, something that is yet to be determined. Prerequisites such as preferred scale, biomass properties, end product requirements, and process integration possibilities will also likely affect process choices.

4. Conclusions

Hydroprocessing of fast pyrolysis bio-oil (FPBO) in fixed bed hydroprocessing reactors has been extensively studied but remains challenging due to coke formation, catalyst deactivation, and pressure drop build-ups. In this work, FPBO was first hydroprocessed in a slurry-process with the aim to facilitate downstream processing in a fixed bed hydrotreater by producing a more stable, partly deoxygenated, bio-oil.

The slurry-process resulted in an oil product with reduced oxygen concentration, improved stability, and low coking tendencies. This product was successfully processed in the downstream fixed bed hydrotreater for 58 h without any notable catalyst deactivation or pressure build-up. The FB-process provided deoxygenated (0.5 wt% oxygen) hydrocarbons, approximately equally divided between gasoline and diesel boiling point ranges. The final oil product was distilled into gasoline and diesel boiling point fractions, and both were shown to have cycloalkanes as the compound group with highest concentration, followed by paraffins and aromatics. The overall process resulted in a 28.7 wt% yield of deoxygenated oil product from the FPBO, and a carbon recovery from FPBO to deoxygenated oil product of 67.7 wt%. Carbon not retained in the oil was lost as gaseous hydrocarbons (13.2 wt%), gaseous carbon oxides (5.4 wt%), and organic compounds in the water product (12.8 wt%), with most of these losses occurring in the slurry-process. The combined H_2 consumption in the two process steps was 52.6 g per kg of processed dry FPBO, or 140 g per kg of produced deoxygenated oil product. The carbon recovery and H_2 consumption were compared with corresponding values obtained in other studies focused on hydroprocessing of bio-based pyrolysis oils and found to agree relatively well. Although promising, further work is required to fully evaluate the feasibility of the process concept. Future work should also strive to determine to what degree FPBO needs to be stabilized and pretreated for downstream processing in fixed bed hydrotreaters to be successful, while also maximizing the carbon recovery in the oil product.

CRediT authorship contribution statement

Niklas Bergvall: Conceptualization, Data curation, Formal analysis, Writing – original draft, Writing – review & editing, Investigation. **You Wayne Cheah:** Data curation, Formal analysis, Investigation, Writing – original draft, Writing – review & editing. **Christian Bernlind:** Data curation, Investigation, Writing – original draft. **Alexandra Bernlind:** Data curation, Formal analysis, Writing – original draft. **Louise Olsson:** Writing – review & editing. **Derek Creaser:** Conceptualization, Writing – review & editing. **Linda Sandström:** Conceptualization, Writing – original draft, Writing – review & editing. **Olov G.W. Öhrman:** Conceptualization, Writing – review & editing.

Declaration of Competing Interest

The authors declare that they have no known competing financial interests or personal relationships that could have appeared to influence the work reported in this paper.

Data availability

Data will be made available on request.

Acknowledgements

This work was funded by the Swedish Energy Agency, project number 41253-2.

Appendix A. Supplementary data

Supplementary data to this article can be found online at https://doi.org/10.1016/j.fuproc.2023.108009.

References

[1] J. Kuylenstierna, C. Hermansson, K. Bäckstrand, A. Nordlund, M. Rummukainen, B. Sanden, P. Söderholm, S. Sörlin, Report of the Swedish Climate Policy Council 2022, 2022.
[2] K. Jacobson, K.C. Maheria, A.K. Dalai, Bio-oil valorization: a review, Renew. Sust. Energ. Rev. 23 (2013) 91–106.
[3] A.P.P. Pires, J. Arauzo, I. Fonts, M.E. Domine, A.F. Arroyo, M.E. Garcia-Perez, J. Montoya, F. Chejne, P. Pfromm, M. Garcia-Perez, Challenges and opportunities for bio-oil refining: a review, Energy Fuel 33 (2019) 4683–4720.
[4] P. Mäki-Arvela, D. Murzin, Hydrodeoxygenation of lignin-derived phenols: from fundamental studies towards industrial applications, Catalysts 7 (2017) 265.
[5] V. Paasikallio, C. Lindfors, E. Kuoppala, Y. Solantausta, A. Oasmaa, J. Lehto, J. Lehtonen, Product quality and catalyst deactivation in a four day catalytic pyrolysis production run, Green Chem. 16 (7) (2014) 3549–3559.
[6] D.C. Makepa, C.H. Chihobo, W.R. Ruziwa, D. Musademba, A systematic review of the techno-economic assessment and biomass supply chain uncertainties of biofuels production from fast pyrolysis of lignocellulosic biomass, Fuel Commun. 14 (2023), 100086.
[7] Y. Han, M. Gholizadeh, C.-C. Tran, S. Kaliaguine, C.-Z. Li, M. Olarte, M. Garcia-Perez, Hydrotreatment of pyrolysis bio-oil: a review, Fuel Process. Technol. 195 (2019), 106140.
[8] D.R. Parapati, V.K. Guda, V.K. Penmetsa, P.H. Steele, S.K. Tanneru, Single stage hydroprocessing of pyrolysis oil in a continuous packed-bed reactor, Environ. Prog. Sustain. Energy 33 (2014) 676–680.
[9] D.C. Elliott, T.R. Hart, G.G. Neuenschwander, L.J. Rotness, M.V. Olarte, Catalytic hydroprocessing of fast pyrolysis bio-oil from pine sawdust, Energy Fuel 26 (2012) 3891–3896.
[10] D.C. Elliot, Catalytic Hydroprocessing of Bio-Oils of Different Types. Ph.D. Thesis, University of Groningen, Groningen, Netherlands, 2019.
[11] T. Janosik, A.N. Nilsson, A.C. Hällgren, M. Hedberg, C. Bernlind, H. Rådberg, L. Ahlsén, P. Arora, O.G.W. Öhrman, Derivatizing of fast pyrolysis bio-oil and coprocessing in fixed bed hydrotreater, Energy Fuel 36 (2022) 8274–8287.
[12] P. Lahijani, M. Mohammadi, A.R. Mohamed, F. Ismail, K.T. Lee, G. Amini, Upgrading biomass-derived pyrolysis bio-oil to bio-jet fuel through catalytic cracking and hydrodeoxygenation: a review of recent progress, Energy Convers. Manag. 268 (2022), 115956.
[13] X. Hu, Z. Zhang, M. Gholizadeh, S. Zhang, C.H. Lam, Z. Xiong, Y. Wang, Coke formation during thermal treatment of bio-oil, Energy Fuel 34 (2020) 7863–7914.
[14] A.H. Zacher, D.C. Elliott, M.V. Olarte, H. Wang, S.B. Jones, P.A. Meyer, Technology advancements in hydroprocessing of bio-oils, Biomass Bioenergy 125 (2019) 151–168.
[15] D.C. Elliot, Historical developments in hydroprocessing of bio-oils, Energy Fuel 21 (3) (2007) 1792–1815.
[16] A. Oasmaa, J. Lehto, Y. Solantausta, S. Kallio, Historical review on VTT fast pyrolysis bio-oil production and upgrading, Energy Fuel 35 (7) (2021) 5683–5695.
[17] Y. Yang, X. Xu, H. He, D. Huo, X. Li, L. Dai, C. Si, The catalytic hydrodeoxygenation of bio-oil for upgradation from lignocellulosic biomass, Int. J. Biol. Macromol. 242 (2023), 124773.
[18] D. Santosa, I. Kutnyakov, M. Flake, H. Wang, Coprocessing biomass fast pyrolysis and catalytic fast pyrolysis oils with vacuum gas oil in refinery hydroprocessing, Energy Fuel 36 (2022) 12641–12650.
[19] C. Lindfors, D.C. Elliott, W. Prins, A. Oasmaa, J. Lehtonen, Co-processing of biocrudes in oil refineries, Energy Fuel 37 (2023) 799–804.
[20] N. Bergvall, L. Sandström, F. Weiland, O.G.W. Öhrman, Corefining of fast pyrolysis bio-oil with vacuum residue and vacuum gas oil in a continuous slurry hydrocracking process, Energy Fuel 34 (7) (2020) 8452–8465.
[21] N. Bergvall, R. Molinder, A.-C. Johansson, L. Sandström, Continuous slurry hydrocracking of biobased fast pyrolysis oil, Energy Fuel 35 (3) (2021) 2303–2312.
[22] A.-C. Johansson, N. Bergvall, R. Molinder, E. Wikberg, M. Niinipuu, L. Sandström, Comparison of co-refining of fast pyrolysis oil from Salix via catalytic cracking and hydroprocessing, Biomass Bioenergy 172 (2023), 106753.
[23] Y. Zhang, J. Monnier, M. Ikura, Bio-oil upgrading using dispersed unsupported MoS2 catalyst, Fuel Process. Technol. 206 (2020), 106403.
[24] N. Bergvall, L. Sandström, Y.W. Cheah, O.G.W. Öhrman, Slurry hydroconversion of solid Kraft lignin to liquid products using molybdenum- and iron-based catalysts, Energy Fuel 36 (2022) 10226–10242.
[25] A. Dimitriadis, N. Bergvall, A.-C. Johansson, L. Sandström, S. Bezergianni, N. Tourlakidis, L. Meca, P. Kukula, L. Raymakers, Biomass conversion via ablative fast pyrolysis and hydroprocessing towards refinery integration: industrially relevant scale validation, Fuel 332 (2023), 126153.
[26] A. Dimitriadis, G. Meletidis, U. Pfisterer, M. Auersvald, D. Kubička, S. Bezergianni, Integration of stabilized bio-oil in light cycle oil hydrotreatment unit targeting hybrid fuels, Fuel Process. Technol. 230 (2022), 107220.
[27] M.A. Salam, Y.W. Cheah, P.H. Ho, D. Bernin, A. Achour, E. Nejadmoghadam, O.G. W. Öhrman, P. Arora, L. Olsson, D. Creaser, Elucidating the role of NiMoS-USY during the hydrotreatment of Kraft lignin, Chem. Eng. J. 442 (2) (2022), 136216.
[28] G. Bagnato, A. Sanna, E. Paone, E. Catizzone, Recent catalytic advances in hydrotreatment processes of pyrolysis bio-oil, Catalysts 11 (2021) 157.
[29] E. Laurent, B. Delmon, Study of the hydrodeoxygenation of carbonyl, carboxylic and guaiacyl groups over sulfided Como/gamma-al2o3 and Nimo/gamma-al2o3 catalysts. 1. Catalytic reaction schemes, Appl. Catal. A Gen. 109 (1) (1994) 77–96.
[30] J.P.A. Diebold, A Review of the Chemical and Physical Mechanisms of the Storage Stability of Fast Pyrolysis Bio-Oils, NREL/SR-570-27613, National Renewable Energy Laboratory, Golden, CO, USA, 1999.
[31] A. Oasmaa, J. Korhonen, E. Kuoppala, An approach for stability measurement of wood-based fast pyrolysis bio-oils, Energy Fuel 25 (7) (2011) 3307–3313.
[32] M. Broumand, M.S. Khan, S. Yun, Z. Hong, M.J. Thomson, The effect of thermo-catalytic reforming of a pyrolysis bio-oil on its performance in a micro-gas turbine burner, Appl. Energy Combust. Sci. 5 (2021).
[33] W. Yin, Z. Wang, H. Yang, R.H. Venderbosch, H.J. Heeres, Catalytic hydrotreatment of biomass-derived fast pyrolysis liquids using Ni and Cu-based PRICAT catalysts, Energy Fuel 36 (23) (2022) 14281–14291.
[34] B. Shumeiko, M. Auersvald, D. Vrtiška, P. Straka, P. Šimáček, I. Svetlik, S. Bezergianni, D. Kubička, Reduction of fossil CO2 emissions of engine fuels by integration of stabilized bio-oil distillation residue to a crude-oil refinery hydrocracking process, Chem. Eng. J. 465 (2023), 142899.
[35] E.D. Christensen, G.M. Chupka, J. Luecke, T. Smurthwaite, T.L. Alleman, K. Iisa, J. A. Franz, D.C. Elliott, A.R.L. McCormick, Analysis of oxygenated compounds in hydrotreated biomass fast pyrolysis oil distillate fractions, Energy Fuel 25 (11) (2011) 5462–6471.
[36] S.K. Sahoo, S.S. Ray, I. Singh, Structural characterization of coke on spent hydroprocessing catalysts used for processing of vacuum gas oils, Appl. Catal. A Gen. 278 (1) (2004) 83–91.
[37] N.T. Nguyen, K.H. Kang, P.W. Seo, N. Kang, D.V. Pham, C. Ahn, G.T. Kim, S. Park, Hydrocracking of C5-isolated asphaltene and its fractions in batch and semi-batch reactors, Energies 13 (2020) 4444.
[38] M. Gholizadeh, R. Gunawan, X. Hu, F.D.M. Mercader, R. Westerhof, W. Chaitwat, M.M. Hasan, D. Mourant, C.-Z. Li, Effects of temperature on the hydrotreatment behaviour of pyrolysis bio-oil and coke formation in a continuous hydrotreatment reactor, Fuel Process. Technol. 148 (2016) 175–183.
[39] A. Oasmaa, Y. Solantausta, V. Arpiainen, E. Kuoppala, K. Sipilä, Fast pyrolysis bio-oils from wood and agricultural residues, Energy Fuel 24 (2) (2010) 1380–1388.
[40] D. Elliott, H. Wang, R. French, S. Deutch, K. Iisa, Hydrocarbon liquid production from biomass via hot-vapor filtered fast pyrolysis and catalytic hydroprocessing of the bio-oil, Energy Fuel 28 (2014) 5909–5917.
[41] F.A. Agblevor, D.C. Elliott, D.M. Santosa, M.V. Olarte, S.D. Burton, M. Swita, S. H. Beis, K. Christian, A.B. Sargen, Red mud catalytic pyrolysis of pinyon juniper and single-stage hydrotreatment of oils, Energy Fuel 30 (2016) 7947–7958.
[42] W. Yin, H. Gu, M.B. Figueirêdo, S. Xia, R.H. Venderbosch, H.J. Heeres, Stabilization of fast pyrolysis liquids from biomass by catalytic hydrotreatment using Raney nickel "type" catalysts, Fuel Process. Technol. 219 (2021), 106846.